International Journal of Enhanced Research in Science, Technology & Engineering
ISSN: 2319-7463, Vol. 7 Issue 11, November-2018, Impact Factor: 4.059

To Combat Food Fraud, Use Plant Physiological Stable Oxygen Isotope Models

Shalini Saxena

Laboratory of Cytogenetics Department of Botany Bareilly College, Bareilly, U.P, India

INTRODUCTION

Food fraud causes $30 to $40 billion in economic losses each year, particularly when bogus geographic origin claims are involved. The most effective forensic procedures for locating these crimes use stable isotope techniques, including those that use oxygen isotopes (δ18O). Stable oxygen isotope models for plants simulate how climatic factors and precipitation δ18O values affect the δ18O values of water and organic molecules in plants. These models have the ability to streamline, expedite, and enhance traditional stable isotope applications as well as generate temporally resolved, accurate, and precise region-of-origin assignments for agricultural foods. However, the implementation of the models for the origin identification of food has been constrained by the validation of these models and, consequently, the optimal selection of model parameters and input variables.

In our work, we compare model predictions to a unique 11-year European strawberry δ18O reference dataset to assess how the parameterization of the model and the choice of variable input sources affect the model's predictive capability. Our findings demonstrate that plant physiological isotope models provide a novel and dynamic approach that can precisely predict the geographic origin of a plant product and can advance the field of stable isotope analysis to combat food fraud by modifying leaf-based model parameters specifically for fruit and with product-independent but growth time-specific environmental input data.

Food fraud, which is the deliberate and deceptive adulteration of food for financial advantage, is thought to cost up to $40 billion annually4-6. 10% to 30% of all commercially sold food is thought to be fake, even though most incidents go unreported4,5. Food fraud is most frequently committed by inaccurately reporting the nation of origin, which is done to save costs and increase profits. This damages customer confidence and raises the possibility of decreased quality and health risk. Therefore, there is a strong demand for analytical instruments for the independent verification of food's geographic origin.

Stable isotope analyses are one of the primary techniques for forensically determining the geographic origin of food. Since the climate and topography, the underlying geology, and agricultural practices produce location-specific isotopic fin- fingerprints in a product, stable isotopes are particularly well suited for determining the origin of agricultural products. The majority of techniques for determining the origin of a sample using stable isotopes rely on a direct comparison of the sample's isotopic fingerprint to genuine reference material with a known origin. For these comparisons, statistical analysis is simple, and data interpretation is simple for both customers and law enforcement agencies.

However, gathering genuine reference samples takes time and money, particularly on a worldwide scale. Therefore, it is difficult to account for the inter- and intra-annual variability observed in plant oxygen and hydrogen isotope composition, the two stable isotope ratios that are usually utilized for origin analyses. Large reference datasets are frequently geographically dispersed and temporally not sufficiently resolved. The forecast of agricultural goods' provenance may become significantly more uncertain as a result of this restriction.

In this paper, we show that mechanistic stable oxygen isotope models of plant physiology can be parametrized to provide a quick, logistically straightforward, and inexpensive substitute for determining the provenance of agricultural plant products. The local precipitation's δ18O values and the plant's evaporative environment, both of which exhibit distinct regional patterns, determine the oxygen isotope composition (δ18O) of organic molecules in plants.

Plant physiological stable isotope models may simulate how climatic factors and precipitation water δ18O values work together to shape the δ18O values of water inside the plant and how these plant water δ18O values are imprinted into the organic elements of the plant. Therefore, mechanistic plant physiological stable oxygen isotope models may be able to mimic the regional variation.

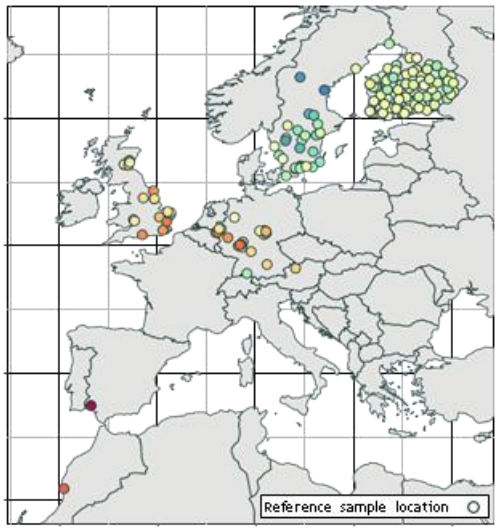

Image. The locations of the 154 real reference samples used for model validation are depicted on a map of Europe. The samples were taken from 2007 to 2017.

The measured δ18O values of the strawberry bulk-dried tissue from the reference samples are displayed in the colored fill of the dots. The majority of the samples were taken between May and July 1976, which was the peak strawberry season in Europe. R, version 3.5.3, which may be downloaded at https://www.r-project.org, was used to make the map. plant δ18O values, to which δ18O readings of allegedly contaminated food samples can be compared and their alleged geographic provenance confirmed.

We use a special Europe-wide strawberry δ18O reference dataset that contains 154 genuine reference samples that have been collected throughout Europe from 2007 to 2017 (Fig. 1) to conceptually illustrate how a mechanistic plant physiological stable isotope model can be used to simulate the geographic variability in δ18O values of food products. We use this dataset to verify our model assumptions about model parameters and model input variables as well as to evaluate our model predictions across space and time. With this method, we examine whether or not plant physiological stable oxygen isotope models, which were originally created for cellulose or leaf water in the leaves or stems of plants, are generally applicable for determining the country of origin of agricultural products, or whether they require parameterization for particular plant species and their products. Furthermore, we thoroughly assess the kind, essential spatial resolution, and temporal integration of isotopic (precipitation δ18O values) and meteorological (temperature, relative humidity) input variables necessary for the most precise forecast of strawberry δ18O values across Europe.

RESULTS

The two-pool adapted Craig-Gordon model is the foundation for the model we employed in our simulations. To choose the ideal set of model input variables and parameters, we used a two-step process. First, we combined the two main physiological model parameters in various ways. These are pxpex/pxpexc, which calculates the amount of oxygen exchange between sugars and the surrounding plant water during the biosynthesis of cellulose (pxpex) and other compounds (pxpexc), and fxylem, which accounts for the dilution of δ18O enriched water at the site of evaporation in leaves with the plant's source water. We used \

(i) mean values from the literature that were originally established for leaf water (xylem) and leaf cellulose δ18O values (pxpex) across different plant species. Additionally, we utilized values that were particularly established for
(ii) leaf water (fxylem) and bulk dried tissue of berries (pxpexc) in berry-producing plants, as well as
(iii) leaf water (fxylem) and bulk dried tissue of berries (pxpexc) of strawberry plants in particular (see Table 1 and methods for a detailed description of the parameter selection). Since the expert for strawberries and other berry-producing plant species is the same, we only needed one pxpexc value, one pxpex value, three xylem values, and six different parameterized models (Fig. 2a). In a subsequent stage, we used various combinations of environmental model input variables to run these six models with various parameterizations. This includes several precipitation sources.

Prior to the field sample's actual harvest date, δ18O and climatic data, as well as other time frames over which to integrate these data, were collected (Table 2). Each set of model parameters produced unique model simulations depending on the combination of the model's input variables (Fig. 2a). We calculated root mean squared error

(RMSE) values based on the comparison to our reference dataset for each of the combinations of input variables for each of the six parameter combinations in order to assess the performance differences between the various model parameters and variable input options.

We discovered that the δ18O values of strawberry bulk dry material could be accurately predicted by all six distinct parameterized models. Using strawberry-specific model parameters produced the best model performance, with a minimum RMSE of 0.95. With a minimal RMSE of 1.11, even the most broad parameters, however, still performed admirably (Fig. 2). Models that employed at least one general parameter derived from average literature values for leaves underperformed those that used average parameters (xylem and expect) for berry-producing plants or parameters specific to strawberry plants (Fig. 2a,b). The strawberry-specific model parameters (strawberry xylem and berry/strawberry pxpexc) produced the overall best results (Fig. 2a,b). Regardless of the species, the model parameterized with average berry-producing plant attributes consistently performed second best (Fig. 2a,b). The choice of average berry-producing plant or strawberry-specific values for the model parameter xylem instead of the option of pxpex/pxpexc values in particular turned out to be more crucial for improving model performance (Fig. 2a).

Our investigation also showed that, regardless of the parameterization of the model, the choice of model input data has a significant impact on the quality of the model output (Fig. 2c-j). Despite the lower spatial resolution of the CRU data, models using data from the E-OBS dataset (0.1° grid)30 outperformed models using monthly mean temperature from the climatic research unit (CRU) (0.5° grid)29 out of the 65,536 different combinations of input parameter choices we tested (Fig. 2c). Similar results were obtained using relative humidity values generated from CRU vapor pressure data as opposed to E-OBS data (Fig. 2e). The model comparisons also revealed that the input data for temperature and vapor pressure for the month before the collection of a reference sample were used to produce the best predictions (Fig. 2d,f, Supplementary Information dataset S1 to S6). The models employing monthly values from the OIPC31, which are not specific for a certain year, often displayed a better fit than those using Piso (26 out of the 30 lowest RMSEs) for precipitation δ18O data. AI32, which foretells values for particular years and months (Fig. 2g). Nevertheless, Piso.AI's estimated mean of the three months preceding sampling (Supplementary Information dataset S6) served as the foundation for the single best-fit values. However, the chosen data source for vapor δ18O values did not reveal such a distinct trend (Fig. 2i). The choice of the time period prior to the collection of the reference sample did not yield a consistent best choice for the precipitation and vapor δ18O input variables, in contrast to the temperature and vapor pressure data (Fig. 2h,j).

After comparing every model parameter and input data option, we discovered two nearly identical highest performing models.

developing models. The models that used parameters specific to strawberries had an RMSE of 0.95 and the models that used average model input parameters for berry-producing plants had an RMSE of 0.96 (Figs. 2 and 3). The best-performing model for berry-producing plants used monthly air temperature and vapor pressure data from CRU from one month prior to the collection of a reference sample in a particular year, precipitation δ18O values from the precipitation-weighted mean of the three months leading up to the harvest date of a sample from the long term mean monthly values provided by OIPC, and vapor δ18O values calculated under the assumption that isotopic equilibrium with the pre-harvest atmosphere.

For the example month of July 2017, the best-performing average berry model projected strawberry bulk dried tissue δ18O values that ranged from + 31 to + 16 across the European continent (Fig. 3b). The most notable outliers came from eight locations in Germany and Sweden, where the model either over predicted or under predicted the measured δ18O variability by 2.0 to 3.5 times (Fig. 3a). This indicates that the measured δ18O variability within one region was often higher than the variability recorded by the model. Although we obtained strawberry bulk dried tissue δ18O values (1) from berry samples that were collected on the same field and the same day (primarily from Germany and Finland), the model-induced uncertainty mainly fell within the 95% quantile of that variability (Fig. 3a).

DISCUSSION

We show that a stable oxygen isotope model for plants can be a useful tool for forecasting the geographical variability of δ18O values in fruit. This model predicts the δ18O values of organic compounds in leaves and wood. Models parameterized using common across-species averaged leaf-derived values for the model parameters xylem and anticipated can predict observed data with an average RMSE of 1.11 when given the best environmental input data. Model parameters that were particularly determined for strawberry plant leaves (xylem) and berries (apex) were necessary for the model that accurately predicted δ18O values of bulk dried strawberry tissue. However, this model's performance was only slightly better than the best-performing model, which was parameterized with average values for the leaves (xylem) and berries (pxpexc) of berry-producing plants generally (RMSE = 0.95 vs.

RMSE = 0.96). ‰). This shows that for berry-producing plants, employing average parameters will be sufficient for high-quality model performance. The model performs reasonably well even when its parameters are general values calculated for leaves and averaged across various species. An important result of this work is the resilient performance of the models with diverse parameterizations. It implies that the mechanistic stable oxygen isotope model of plant physiology can be applied broadly to simulate the geographic variability of δ18O values in fruit. Our analysis also reveals that the effectiveness of the model depends on the careful selection of model input variables that are specific for the year and month of sample collection-with varied lead durations.

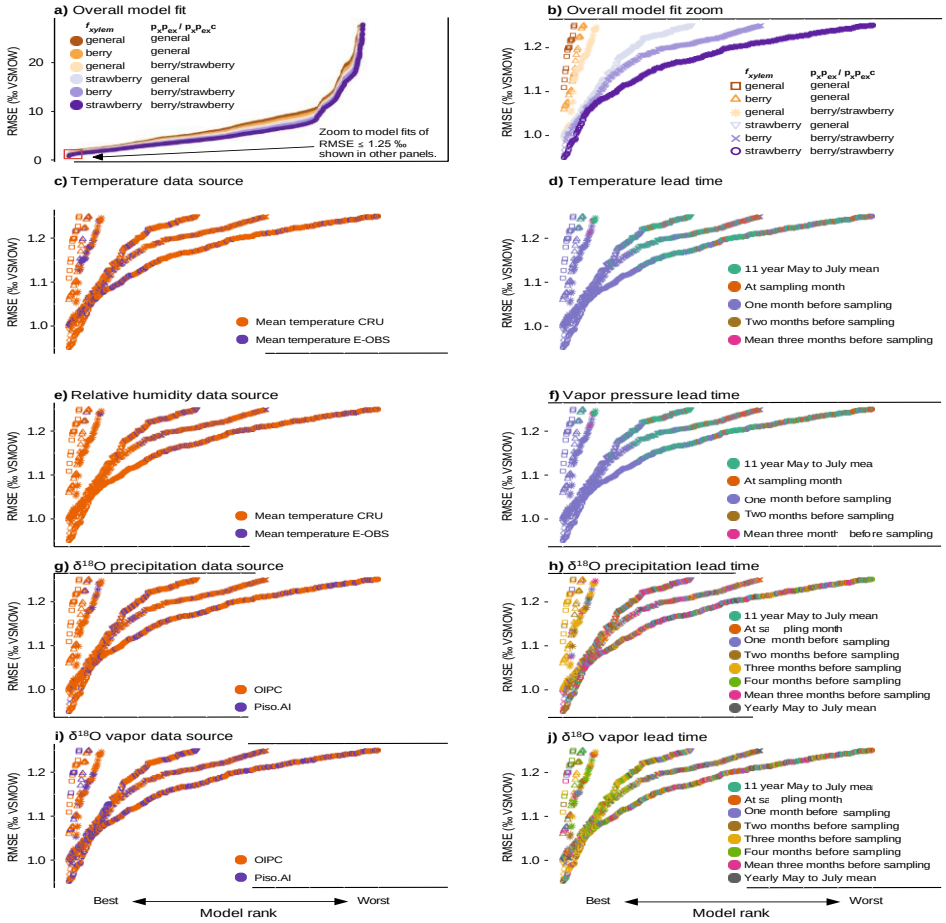

Image 2. Analyses of the model fit for all combinations of parameters and input data. The model's root mean square error (RMSE) values are shown in all panels. They were calculated using a comparison of the observed and modeled bulk-dried tissue δ18O values (n = 154) from reliable reference samples. Each dot corresponds to the RMSE (in VSMOW) resulting from a particular model parameter and input data combination. RMSE values are ranked based on model fit. From the entire set of 65,536 tested possibilities in each of the six different parameterized models (n 14,850 for each parameter combination), Panel (a) displays the sorted RMSE values that are lower than 25. The symbols are colored based on the various model parameter combinations (xylem and pxpex/pxpexc) used for the simulations, either general parameters for leaves averaged across various species using literature values ("general"), parameters that are average values for leaves (xylem) and berries (pxpexc) of plants that produce berries ("berry"), or parameters specifically determined for leaves.

Strawberry plants' berries (apex) and fxylem ("strawberry"). Only the models with RMSE values less than 1.25 are displayed in Panels (b–j).

(Panel a, red square). Symbols for the various model parameter combinations are introduced in panel (b), which displays the ranking model fits for the same model parameter and input data combinations as panel (a). Panels (c-j) continue to use the same symbols. For more information, see the panel in the figures and the datasets S1 to S6 in the Supplementary Information. In panels (c) to (j), the symbols are colored according to the model input data used for the simulation. Comparing the usage of CRU29 and E-OBS30 input data, panels (c) and (e), panels (g), and Panels (d, f, h, and j) compare the use of various lead time intervals preceding the collection date of the reference material (see methods). (i) Compare the usage of OIPC31 to Piso.AI32 isotope data sources. For panels (d) and (f), several time intervals produced RMSE values more significant than the shown range and are therefore not indicated in the legends because the panels only display the best model fits for RMSE values up to 1.25.

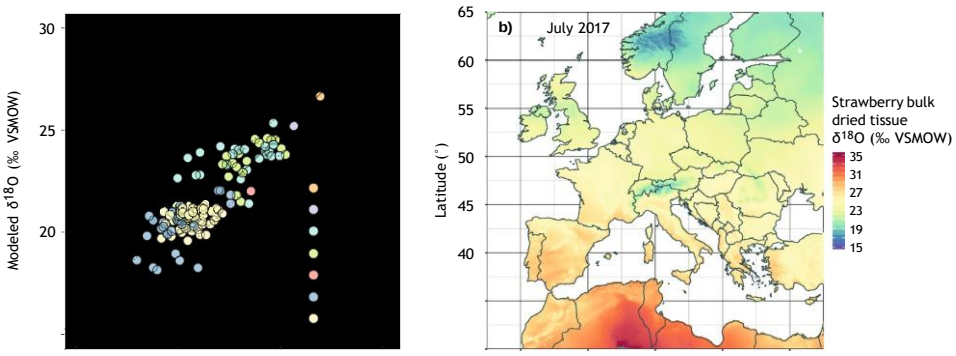

Image 3. Results of applying plant physiological isotope models to simulate the bulk dried δ18O values of berries. (a) The measured actual bulk dried tissue reference samples δ18O values are displayed against the modeled bulk dried tissue δ18O values generated from the model parameterized with general data for berries (n = 154; RMSE = 0.96). The dashed lines display the 95% quantile of the observed within-field variability of strawberry δ18O bulk dried tissue values, and the solid line represents the 1:1 line. (b) A map of Europe displaying the anticipated regional distribution of strawberry bulk dry tissue δ18O values, in this case obtained in July 2017. R, version 3.5.3, was used to build the map (https://www.r-project.org/).

We discovered that model simulations with parameters defined for berry-producing plants (both average across berry-producing plants and strawberry-specific) produced model outputs that were marginally better than those with parameters obtained from averaging leaf-derived literature values across species (Fig. 2). Berries, like the majority of other fruit, rely on sugars imported from active photosynthetic organs (i.e., leaves), making them predominantly heterotrophic (carbon-sink) tissues. These sugars transmit a leaf water δ18O signal that is physiologically and climatically driven21,22,26,33,34. The Craig-Gordon model can calculate this leaf water's δ18O value, which gets imprinted into sugars with a fixed fractionation of +27, if the model is modified to include the parameter xylem, which accounts for the dilution of the evaporatively δ18O-enriched leaf water by the plant's source water35. We used xylem values recently discovered from separate growth chamber tests for strawberry plants (0.30) or berry-producing plants in general (0.26), respectively, for the two best-performing models. These xylem values were marginally higher than the mean values (0.22; 36–40) that were generally reported for leaves from different species in the literature. The average xylem value given by the previously researched plants, which included less productive wild plants with potentially lower transpiration rates, was 0.22. Higher xylem values could be the result of higher transpiration rates in berry-producing plants used in agriculture.

Some of the oxygen in the sugars exchanges with the surrounding water while being transported from leaves through the phloem to carbon-sink tissues like berries and while being synthesized into carbohydrates in the sink tissues41,42. Comparing this water to leaf water43 reveals that it lacks δ18O. As a result, the sugar and carbohydrate levels in sink tissues are different from those of leaves28,44. The parameter expert in the model, among other things, accounts for this effect. Our investigation demonstrates that the match of anticipated strawberry-dried tissue δ18O values to those of reference samples was enhanced by using pxpexc values that are particular to berries in berry-producing plants. The expected value for berry bulk dried tissue was higher than the mean value typically reported for the cellulose of leaves (0.46 vs. 0.4045-49), which we found in separate growth chamber experiments (which are identical for strawberries and berries in general)28. Increased oxygen exchange in sugar with plant source water (pex) during phloem transport from leaves to, as well as during carbohydrate synthesis in the berries, may be the cause of a greater pxpexc value in berries than the pxpex value of leaf-cellulose. Additionally, it is consistent with a recent finding in strawberries and raspberries28 that berries often contain more δ18O-depleted source water than leaves (px). Further, this pattern demonstrates that bulk dried tissue of berries contains compounds with lower δ18O values than cellulose itself50, which is explained by a greater pxpexc value, in comparison to pure cellulose of leaves.

Using the mean air temperature of the coarser spatially resolved models for various parameterized Compared to the higher resolution E-OBS dataset (0.1° grid), the CRU dataset (0.5° grid) produced a better model fit (Fig. 2). Other than the spatial resolution, there are no obvious discrepancies between the two data sources, and the reference samples' E-OBS and CRU mean temperatures correlated with a r2 of 0.81.

For the locations considered in this investigation, 0.98 (y = 1.04x 0.007). We found model prediction skill to be generally better when using long-term monthly climatology-based precipitation δ18O data from the gridded OIPC datasets as input data, as opposed to Piso.AI, even though the best-performing model used precipitation δ18O values from Piso.AI, which uses station coordinates and provides values for single months and years. It is a little unexpected that model fits derived from inputs with lower spatial resolution and climatological data as opposed to

contemporaneous input data were typically more accurate than those produced from inputs that more accurately reflect conditions at any given point in time. This may be related to the fact that the reference samples we utilized as a validation target frequently only have vaguely defined growing locations and collecting dates in the sample metadata (usually only postal codes, region names, and the month in which the lab received the sample). When using the finer products from CRU and OIPC instead of the more finely geographically and temporally resolved E-OBS and Piso.AI products, this may have led to errors in the attribution of climate or precipitation δ18O values from adjacent nearby areas. Additionally, Piso.AI often produces a larger annual cycle than OIPC, so even if choosing the right integration time can lead to a better fit (see best-performing model), choosing the wrong one can have more serious repercussions. OIPC and Piso.AI differ from one other in terms of data sources and integration timeframes. Due to the frequently prolonged residence time of water in soil before plant uptake,51,52 it may be the case that by averaging on interannual timescales, the monthly climatology precipitation δ18O values from OIPC more accurately replicate typical δ18O values of the source water that the plants use. Both procedures have the same result: they even out the extreme δ18O readings that could happen in any given month. If this explanation is accurate, it also suggests that future validation work utilizing fresh reference samples obtained with more exacting metadata may lead to predictions being improved.

Our model output comparison demonstrates that the model's prediction ability was significantly enhanced by incorporating climate input data for a particular year's growing season. This is demonstrated by the improvement in model predictions of the average berry parameterized model when utilizing input data relevant to the growing season (RMSE = 0.96) as opposed to input data averaged over an 11-year period (2007 to 2017) using the mean growing season (RMSE = 1.27). The period preceding sample collection (i.e., during which a product grew) for which climatic input data are averaged before they are fed into the model is crucially important for accurately applying a plant physiological model to simulate δ18O values of bulk dried tissue for any growing season. When simulating the δ18O values in berry bulk dried tissue, we discovered that utilizing average values for air temperature and vapor pressure from one month before to sampling (during the berry's growth) is the most appropriate time period. The fact that climatic drivers of leaf water and consequently bulk dried tissue δ18O values in plants, namely temperature and vapor pressure, can vary significantly from year to year and within a year is the reason for improved model predictions when inter- and intra-annual variability climatic model input variable is taken into account. Because of this, leaf water's δ18O value varies both annually and during the growth season. This temporal variability of plant organic δ18O values at a certain geographic area can be significantly influenced by the inter- and intra-annual variability in leaf water variability values46,53. In contrast to the commonly used reference datasets, which are typically unable to be established for a specific growing season, plant physiological stable isotope models have the option to simulate this variability by using climatic input variables for specific years or specific portions of the growing seasons.

We show how much interannual variability in bulk-dried tissue δ18O levels is caused by the climate.
Assuming that all locations from which real reference samples were gathered in this study can be represented by employing growing season-specific model input variables (Fig. 4). In order to do this, we simulated bulk-dried tissue δ18O values for strawberries for the three months of the growth season (May–July) for each of the 11 years from 2007 to 2017 (33 values per site; see methods for more information on this model simulation). Then, for each sampling point in the resulting 11-year time series, we calculated the widest possible range of values (Fig. 4). According to the data, strawberries' bulk-dried tissue δ18O levels can vary across years by up to 4.10. It's interesting to note that there are different geographical patterns in the interannual variability of bulk dried tissue δ18O values of strawberries, with reduced variability in southern and mid-range latitudes and higher variability in northern latitudes. Site-specific predicted ranges of δ18O readings appeared to follow a latitudinal pattern that was linear and statistically significant (r2 = 0.65, p 0.001). The greater seasonal climate variability in higher latitudes is probably the cause of these varied spatial patterns. Our investigation demonstrates that for the simulation of bulk-dried tissue δ18O values of fruit at higher latitudes, the use of climatic input variables unique to the growth season becomes increasingly important. This uncertainty cannot be resolved by the widely used method of comparing suspect samples of agricultural products that are produced annually to reference data, which is frequently gathered over several years. However, as a workaround for the traditional reference dataset approach, multiple reference datasets may be built up over time for various months.

The temporal selection of precipitation and vapor δ18O data is less than that of the input data from climatic models.
extremely important for faithfully reproducing the measured values. We demonstrate that any combination of precipitation and vapor oxygen isotope input predicts the measured strawberry δ18O bulk dried tissue levels with an accuracy between RMSE values of 0.95 and 0.96 for the best two parameterized models with the best timing of climate. Correspondingly, to 1.17 and 1.20 (Fig. 2 g, i). There is a lag between precipitation and plants' source water δ18O values, according to studies that evaluated the seasonal pattern of precipitation, soil, and plant source water values. There is evidence that plants utilise precipitated water before and, primarily for trees, throughout the growing season51,54,55. According to our findings, the source water for strawberries incorporates precipitation events both before and during the growth of the berry. The model is resilient to variation in the input data for

precipitation and vapor (δ18O) between years, therefore potential anomalies won't significantly affect the model's ability to predict the future. It is significant to highlight that the kind of particular origin analysis that our approach enables requires exact assertions about the location of origin and picking date of the suspicious plant sample in addition to the caliber and timeliness of the model input data. If the berry-specific model input parameters were used, a one-month inaccuracy in the metadata would lower the model's predictive ability due to incorrectly allocated input data, leading to a 0.33-percent higher RMSE. The model application detailed here was created for strawberries produced in open fields, not greenhouses, it should also be noted. Consequently, for a successful analysis, metadata confirming a suspect sample's natural growth circumstances is essential.

The use of the model.

We created prediction maps for δ18O values of bulk dried tissue from three example strawberries collected in July 2017 using the best average berry model to demonstrate the capability of the Craig-Gordon-derived plant physiological isotope model to identify the source of an unknown sample for a specific growing season. This kind of forecast

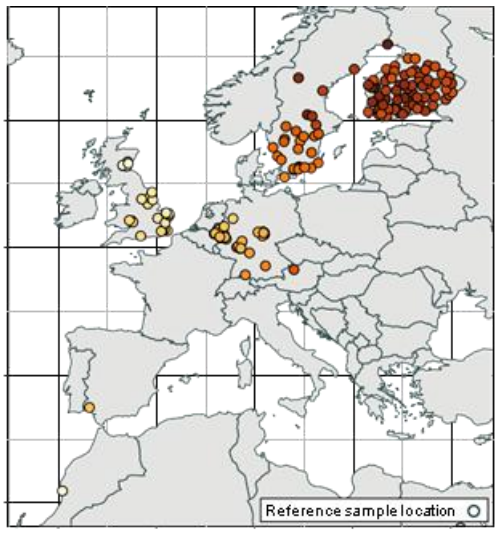

Image 4. Map of Europe displaying the sites where real reference samples were taken, as well as the expected range of strawberry bulk dry tissue δ18O values for each site throughout the entire growing season (May to July) and the years the sample set was taken (2007–2017). The most accurate berry-specific model was used to make predictions (see text). R, version 3.5.3, which may be downloaded at https://www.r-project.org, was used to make the map.

The map is the key item of interest for the forensic food sector since it displays every potential place of origin for an unidentified sample. The simulations demonstrate that it is possible to discriminate between samples from northern Europe, central Europe, and southern Europe. (Fig. 5). The assignment maps also demonstrated that distinct geographic regions may be identified inside numerous different nations. Small areas of south-western France and mid-western Germany (the Cologne Area), for instance, displayed similar δ18O values to those of the southern European samples (Fig. 5c). In this study, we showed that stable oxygen isotope models of plant physiology were capable of producing resolved, accurate, and precise region-of-origin assignments for agricultural food items across time. The isotope-based detection of food fraud will gain from the applicability of model-based region-of-origin assignments for agricultural plant products. The model's robustness and lack of need for species-specific parameterization are two important advantages. This allows the model to be applied, with only minor changes to the model's parameters, to other agricultural plant items or geographical areas in addition to strawberries, which are used here as an example. Although some degree of validation work with genuine samples is required, this ensures that the model may be quickly deployed to constrain the geographic origin of any agricultural plant product.

The model's ability to replicate year- and season-specific δ18O values of a particular plant product and, thus, account for the potentially large temporal variability in such data, is another important advantage. When traditional reference isotope databases are used for origin validation, this is frequently not practicable. Finally, our modeling approach can pinpoint every probable provenance location without the need for significant reference samples over the whole potential region of origin, both in terms of space and time. As a result, it may also be utilized as the main tool to effectively learn about all potential places where a suspicious sample originated and to offer precise guidance on where to gather fresh and/or extra reference samples. Predictions based solely on modeled δ18O values are insufficient to pinpoint the precise growth zone, but they represent a significant improvement over a reference sample-based technique. The potential regions of origin may be even more limited when used in conjunction with

other techniques, such as stable isotope analyses of hydrogen, nitrogen, carbon, or sulfur, which also exhibit distinct geographic patterns depending on underlying bedrock/mineralogy or agricultural practices and have frequently been used in origin determination11,56. These techniques may also be used in conjunction with other authentication techniques, such as proteomics or trace element analysis10. By concealing areas where a specific agricultural plant product cannot be grown or is known not to grow, these strategies can also be improved. As a result, our work demonstrates that combining input data (climate and stable isotope values for precipitation) In addition, plant physiological isotope models present a novel and potent tool that can enhance the use of stable isotopes to combat food fraud.

METHODS

Several references samples. Agroisolab GmbH (Jülich, Germany) provided the real, independent strawberry (Fragaria ananassa) reference samples used in this study's model validation. Between 2007 and 2017, the corporation either directly collected the samples or had approved sample collectors do it on their behalf. Such genuine reference samples are used primarily to directly compare the stable isotope compositions (oxygen, hydrogen, carbon, nitrogen, or sulfur) of the samples to those of unknown provenance. Each reference sample was accompanied by metadata that detailed its geographic origin, such as the community name, postal code, or location coordinates, as well as the month and year the strawberry sample was harvested. We used δ18O readings from 154 reference samples in total. The majority of samples were gathered in Finland, Sweden, the UK, Germany, and Sweden (Fig. 1). Instead of being cultivated in a synthetic greenhouse, all reference samples were grown on strawberry fields that were open to the public. The research complies with all applicable institutional, appropriate national, and international norms and laws. All berry samples were obtained from cultivated, non-endangered plant species (the "garden strawberry").

Samples were collected in the field, stored in airtight containers, and sent right away to Agroisolab, where they were frozen before being analyzed. Dichloromethane was used to solvent-extract the lipids for at least 4 hours using a Soxhlet extractor in order to examine the oxygen-stable isotope composition of the organic strawberry tissue. The remaining samples were ground into a fine powder after being dried. The powder, 1.5 milligrams, was measured into silver capsules. The silver capsules were acclimated in a desiccator with a fixed relative humidity of 11.3% for at least 12 hours. After additional vacuum drying, the samples were analyzed using an isotope-ratio mass spectrometer (IRMS) Horizon from NU Instruments in conjunction with a high-temperature furnace (Hekatech, Wegberg, Germany). The pyrolysis temperature was 1530 °C, and the covalently bonded SiC used in the pyrolysis tube was patented by Agroisolab. The measurement's repeatability was superior than 0.6%.

Calculation using the oxygen isotope model. The oxygen isotopic composition of leaf water or organic compounds produced therein is simulated by plant physiological stable isotope models as δ18O values in per mil (), where δ18O = (δ18O/16O)sample/(δ18O/16O)VSMOW 1 and VSMOW is Vienna Standard Mean Ocean Water as determined by the VSMOW-Standard Light Antarctic Precipitation (SLAP) scale. Modeling plant water δ18O values23,58 is based on the Craig-Gordon model57, which was created to quantitatively characterize the isotopic enrichment of standing water bodies during evaporation and later modified for plants. The baseline for the model is plant source water, which is the soil water derived from precipitation that plants absorb through their roots without isotope fractionation.

$$\text{◆}^{18}O_{e\ leaf} = 1 + \varepsilon^{+} \quad (1 + \varepsilon_k)(1 - e_a/e_i) + e_a/e_i(1 + \text{◆}^{18}O_{Vapor}) \ -1$$

$$\varepsilon^{+} = \exp \quad \frac{1.137}{} * 10^3 - \frac{0.4156}{} - 2.0667 * 10^{-3} \ - 1 \ * 1000 \qquad (2)$$

$$\varepsilon = \frac{28r_s + 19r_b}{}^{k}\, r_s + r_b$$

Where + is the equilibrium fractionation between liquid water and water vapor, k is the kinetic fractionation connected to the diffusion via the stomata and the boundary layer, and δ18Oe_leaf is the oxygen isotope enrichment above the water source at the evaporative location in leaves. The ea/ei ratio compares the intercellular vapor pressure within a leaf to the ambient vapor pressure in the atmosphere. The ambient vapor above the source water, which in this study is considered to be in equilibrium with the source water (δ18OV = +)62,63, is known as δ18OVapor. If the atmosphere is evenly mixed and the supply water for the plants comes from recent precipitation events, this supposition can be applied. Typically, this is the case for crops that are grown in the temperate temperature of the mid-latitudes, particularly for the lengthy (several weeks) strawberry growth season. This assumption should be reevaluated 64 if a similar model is used in other climate zones, such as the tropics. Equations 2 and 3 can be used to derive the equilibrium fractionation factor (+)65,66 and kinetic fractionation factor (k)67.

Where T is the leaf temperature in degrees Celsius. In our calculations, leaf temperature was set to 90% of the monthly mean air temperature, which describes a realistic leaf-energy balance scenario for well-watered crops 68,69 and also produced the best model performance with respect to the reference data. As leaf-to-air temperature differences strongly influence leaf water δ18O values, this assumption needs to be independently tested in future applications. For instance, Chan and colleagues used their model to predict the effects of temperature on leaf water content. We consistently utilized stomatal conductance values of 0.4 mol/m2s and stomatal resistance values of 1 m2s/mol70 for our model calculations, where rs is the stomatal resistance and rb is the boundary layer resistance in m2s/mmol, the inverse of the stomatal and boundary layer conductance.

Because the model describes the δ18O values of water at the evaporation site while measurements typically give bulk leaf water δ18O values36,71, the Craig-Gordon model's predicted leaf water values are frequently enriched in δ18O relative to measured bulk leaf water δ18O values26,27. The two-pool modification to the Craig-Gordon model corrects this effect by separating bulk leaf water into a pool of evaporatively enriched water at the site.

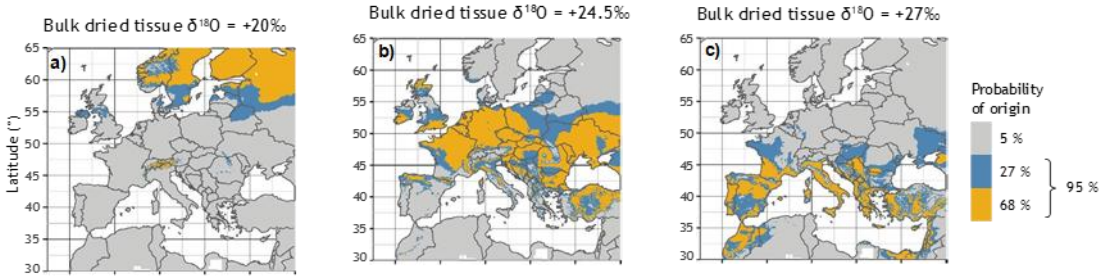

Figure 5 illustrates the prediction maps of three strawberry samples from unknown origins that were gathered in July 2017. The prediction model is based on the best berry-specific model (Fig. 3) and displays the likelihood of origin (greater than 32% in yellow, 5% to 32% in blue, and lower than 5% in grey). Bulk dry tissue Sample's δ18O value is (a) + 20

$$\delta^{18}O_{leaf\ water} = 1 - f_{xylem} * \delta^{18}O_{e\_leaf} + f_{xylem} * \delta^{18}O_{source\ water}$$

$$\delta^{18}O_{e\_leaf} = (\text{﷐}^{18}O_{e\_leaf} + \delta^{18}O_{source\ water}) + (\text{﷐}^{18}O_{e\_leaf} * \delta^{18}O_{source\ water})/1000)$$

$$\delta^{18}O_{cellulose} = p_x p_{ex} * \delta^{18}O_{source\ water} + \varepsilon_{wc} + 1 - p_x p_{ex} * \delta^{18}O_{leaf\ water} + \varepsilon_{wc}$$

$$\delta^{18}O_{bulk} = p_x p_{ex} c * \delta^{18}O_{source\ water} + \varepsilon_{wc} + 1 - p_x p_{ex} c * \delta^{18}O_{leaf\ water} + \varepsilon_{wc}$$

+ 24.5 (mean German sample), (c) + 27 (mean southern European sample), and (mean Finish/Swedish sample). The best berry-specific model's mapped findings were subtracted from the prediction maps to get the δ18O values of the bulk dried tissue of the suspected sample. As a result, a map with a value of zero was produced, illustrating the locations where the sample's δ18O values are expected to be found. The likelihood of the sample's provenance decreases as the size of the discrepancy displayed on the map increases. The one-sigma (68%, yellow) and two-sigma (95%, yellow and blue) confidence intervals around the areas exhibiting no difference to the δ18O value of the suspected sample can be given based on the prediction error of the best berry-specific model (RMSE = 0.96). R, version 3.5.3, was used to produce the three maps (https://www.r-project.org/).

Using unenriched plant source water (δ18Osource water)25 and a pool of evaporation (δ18Oe_leaf generated from the Craig-Gordon model, Eq. 1), δ18Oe_leaf is computed as follows:

In leaf water, xylem concentrations typically range from 0.10 to 0.3336-40, while greater concentrations have also been recorded 72.

Recent research has revealed that the leaf water xylem values for strawberry plants range between 0.24 and 0.3428. The bulk leaf water's δ18O values as well as extra isotopic effects from the digestion of carbohydrates and post-photosynthesis processes are often reflected in the organic molecules in leaves21,22,34. The fractionations take place during the primary digestion of carbohydrates (trioses and hexoses), when carbonyl-group oxygen exchanges with leaf tissue water42. This procedure results in δ18O enrichment, also known as wc42 and measured to be + 27 21,22,73.

When sucrose molecules are converted to glucose and then rejoined during the production of cellulose from primary assimilates, some of the oxygen in the carbonyl group can then exchange with water in the growing cell.

The isotope fractionation (wc) during this procedure is thought to be identical to that during the carbonyl oxygen exchange during primary carbohydrate absorption (+ 27)41,42. The water in the growing cell33 thus partially modifies the δ18O values of the primary assimilate during the synthesis of cellulose. This procedure is described in equation (6).

Where px is the percentage of unenriched source water in the bulk water of the cell where cellulose is synthesized33, sex is the fraction of carbonyl oxygen in cellulose that exchanges with the medium water during synthesis, and δ18Ocellulose is the oxygen isotopic composition of cellulose. It has been discovered that bulk water in growing cells, specifically in the leaf growth-and-differentiation zone, where cellulose is generated, predominantly reflects the isotopic composition of source water43. Consequently, px in Eq. In Eq, 6 is probably bigger than the xylem. (5). For practical reasons, px or pex are often determined as the combined parameter pxpex45 rather than separately. Pxpex was discovered to range from 0.25 to 0.5445-49 for cellulose in grass, crop, and tree leaves.

We try to imitate the δ18O values of dried bulk tissue in this work, as in many applicable situations where plant δ18O values are employed for origin analysis. In addition to carbs, bulk dried plant tissue (δ18Obulk) also contains substances including lignin, lipids, and proteins that may be δ18O-depleted in comparison to carbohydrates50. We added the parameter c because the model must take this into account. We employ pxpex and c as a combined model parameter in our method because they cannot be determined independently.

According to Cueni et al. (in review), there was no statistically significant difference between the strawberry's pure cellulose and bulk dry tissue δ18O levels. Consequently, for strawberries, pxpex and pxpexc are equivalent and range from

	f_{xylem}	$p_x p_{ex}/p_x p_{ex} c$
General	0.22	0.40
Berry	0.26	0.46
Strawberry	0.30	0.46

Table 1. fxylem and pxpex/pxpexc parameter values for the strawberry bulk dried tissue simulations' δ18O values. 0.41 to 0.51. In the context of the data set utilized in this investigation, this method enables the calculation of bulk dry tissue δ18O values without knowledge of δ18O values for cellulose. The method used by Barbour & Farquhar (2000), in contrast, determines the bulk dried tissue's δ18O values by applying an offset (cp) to the cellulose's δ18O values.

choosing a model's parameters. We used several combinations of the parameter values to determine the best values for the major model parameters for the prediction of strawberry bulk dried tissue δ18O levels. To determine whether a leaf-level parameterization of the model is sufficient or whether a berry-specific parameterization is required for producing a satisfying model prediction, we specifically compared average parameter values from the literature derived from leaves and parameter values explicitly derived for berries (Cueni et al. in review). These values were either (i) averaged fxylem and pxpex values from various species reported in the literature for leaf water and cellulose, (ii) averaged fxylem and pxpexc values from berry-producing plants, or (iii) values for fxylem and pxpexc specifically obtained from strawberry plants. For leaf water and leaf, we utilized mean literature values that were initially acquired.

The mean leaf-derived xylem value for berries (average of the values of raspberries and strawberries) was 0.26, and the value for pxpexc was found to be 0.46 (Table 1) (data derived from Cueni et al. in review). We used a leaf-derived xylem value of 0.30 for strawberry plants, and we calculated a value of 0.46 for bulk dry tissue (pxpexc) (data derived from Cueni et al. in review) (Table 1). There were a total of six distinct model input parameter combinations because different berry species' pxpexc values were identical.

Selection of input data for environmental models. Spatial gridded climate and precipitation isotope data layers were used as model inputs to spatially apply the strawberry parametrized bulk-dried tissue oxygen model. However, employing the best and most appropriate input variables is necessary for the correct modeling of geographically different δ18O values. Therefore, we investigated the significance of the input data's temporal averaging and lead time in relation to the berry's picking date. These were referred to as the "integration time" of the input data altogether. It has been demonstrated that plant tissue water and organic compound δ18O values are influenced by the growing season's climate46,53 and precipitation δ18O values of rain events before and during the growing season51,54,55. Thus, determining the best type and integration time of model input variables required for this kind of model simulation was the main goal of our work. Additionally, we employed a variety of spatial climate and precipitation isotope datasets in our analyses to select the best data source (Table 2).

The mean monthly precipitation δ18O grids by Bowen (2015), which are updated versions of the grids made by Bowen and Revenaugh (2003) and Bowen et al. (2005) (Online Isotopes in Precipitation Calculator, OIPC Version

3.2), were compared with one another. They give monthly long-term mean precipitation isotope readings in the form of global grids. These worldwide grids have a resolution of 5'. (2) Piso.AI (Version 1.01)32 forecasts for precipitation isotopes. In accordance with station coordinates 32, this source offers values for specific months and years. On the one hand, we treated both data sets as two separate, independent input data sets and used them for the precipitation δ18O input data of the model as well as to extrapolate the vapor δ18O values from sets (see model description above).

We used the gridded data products from the Climatic Research Unit (CRU) (TS Version 4.04)29 and the E-OBS gridded dataset by the European Climate Assessment & Dataset (Version 22.0e)30 for the climatic drivers of the model (air temperature and vapor pressure) (Table 2). The CRU dataset offered 0.5°-resolution global gridded monthly mean air temperature and mean vapor pressure. The daily mean air temperature and relative humidity for Europe were gridded and had a resolution of 0.1 arc-degrees in the E-OBS dataset. On the basis of these daily mean air temperature and relative humidity grids, we created monthly mean air temperature and grid layers.

Prior to plucking, fruit tissue is formed over a period of weeks46,53. As a result, there is a lag time between the selection date and the date that most accurately captures the source water and vapor stable isotope signal impacting the isotope signal during tissue formation. We therefore looked into lead times of 1, 2, 3, and 4 months as well as the three months before to the selection date as the integration time of the input data (Table 2). Furthermore, we also utilized more general European strawberry growing season averages76, which were not dependent on the sampling year or the sampling month (annual May to July mean; Table 2). Using CRU mean monthly precipitation data, precipitation isotope data were derived as amount-weighted averages. This indicates that the long-term mean precipitation δ18O values obtained from OIPC were weighted using average monthly precipitation totals (May, June, and July) and yearly specific CRU monthly precipitation totals for the case of the three months or growing season averages for individual years.

(a) Data products	
Input variable	**Data product sources**
Climate (Air temperature, vapor pressure/ RH)	CRU, E-OBS
$\delta^{18}O$-precipitation	OIPC, Piso.AI
$\delta^{18}O$-vapor	OIPC, Piso.AI
(b) Integration times	
Name	**Explanation**
At month of sampling	Value of the variable from the month of sample collection
One month before sampling	Value of the variable from one month prior to sample collection
Two months before sampling	Value of the variable from two months prior to sample collection
Three months before sampling	Value of the variable from three months prior to sample collection
Four months before sampling	Value of the variable from four months prior to sample collection
Mean three months before sampling	Average value of the variable from the three months prior to sample collection (precipitation and vapor $d^{18}O$ values are amount-weighted using CRU precipitation totals)
11 year May to July mean	Average value of the variable from the growing season (May to July) averaged over the 11-year period from which samples used in this study were collected
Yearly May to July mean	Average value of the variable from the growing season (May to July) of sample collection

June and July) for the long-term growth season computation from 2007 to 2017. The same evaluation was also done using Piso's precipitation values. AI.

model validation using reference samples. We determined the strawberry bulk dry tissue δ18O values for the location and growing period of each real reference sample using the plant physiological model discussed above. We evaluated all combinations of the data sources listed in Table 2 and each of the eight integration times mentioned in Table 1 for the model input data. The resulting 65,536 input variable combinations for each pair of model parameters (fxylem and pxpex/pxpexc, Table 1) produced model outputs that could be compared to observed reference samples. Our strategy can be explained by the equation given below:

Where s is the data product for the selected input variable (Table 2), t is the integration period of the stated variable (Table 2), and δ18O plant is the simulated δ18O value of the strawberry.

For the key model parameters fxylem and pxpex/pxpexc, we used the average of the values for raspberries and strawberries as well as strawberry-specific values found in Cueni et al.'s (in review) research. For pxpex, we used the values suggested for leaves by the literature. An average value of +27 (wc) was utilized in all calculations. Site-specific elevation was retrieved from the ETOPO1 digital elevation model77 and used to determine the approximate atmospheric pressure in order to derive mean monthly relative humidity values from the given CRU vapor pressure data. Following Buck (1981), these values were added to the air temperature to calculate the saturation vapor pressure (relative humidity = vapor pressure/saturation vapor pressure), which was then used to get the relative humidity. The model's R-script is accessible on "figshare"; the URL is listed in the data availability statement.

Analyses using statistics. The statistical package R, version 3.5.379, was used to conduct the statistical studies. A linear regression model with an alpha level of 0.05 was used to compare the correlations between the range of observed δ18O values and latitude, as well as between the mean air temperatures measured by CRU and E-OBS. The outputs of the 65,536 models were compared with the observed δ18O bulk dry tissue values of the real reference samples (n = 154) using the root mean squared error (RMSE). This was done for each of the six physiological parameter combinations.

prediction map computation. The forensic food industry has developed prediction maps that depict the potential geographic origins of samples with unknown provenance. We created the prediction maps that are displayed in Fig. Here are three examples of strawberry δ18O values from July 2017: (i) + 20 for a typical Finnish/Swedish sample, (ii) + 24.5 for a typical German sample, and (iii) + 27 for a typical southern European sample.

A two-step process was used to calculate the prediction maps. First, we created a map of the anticipated bulk dry tissue δ18O strawberry values for berries harvested in July 2017. We used the average berry model input parameters (xylem and pxpexc, Table 1), as well as the model input data and integration time combination that fit the data the best (Fig. 2), which we evaluated earlier. Thus, we utilized the June 2017 CRU mean air temperature, vapor pressure, and precipitation δ18O values from OIPC, as well as vapor δ18O values calculated using April OIPC precipitation δ18O measurements. This algorithm produced a mapped model result since it used spatial maps as model input data. The prediction maps were computed in the subsequent step. To do this, we first deducted the δ18O value of the sample strawberry's bulk dried tissue from the best berry-specific model's projected result. This was carried out for each map pixel value. A map was created as a consequence, displaying the discrepancy between each map pixel's actual and anticipated δ18O values. Therefore, a value of zero is used to indicate the locations (pixels) projected to have the same δ18O value as the sample strawberry. The one-sigma (68%) and two-sigma (95%) confidence intervals around the areas exhibiting no difference to the δ18O value of the suspicious sample could be evaluated based on the prediction error of the best berry-specific model (RMSE = 0.96). This indicates that the sample's likelihood of provenance decreases as the difference between the sample value and the simulated value of δ18O increases. In other words, a difference of 0 to 0.96 between the sample's δ18O value and the projected δ18O value indicates a possible provenance of at least 68% (one sigma), while a difference of 0.96 to 1.92 indicates a possible provenance of 68 to 27% (two sigmas). Regions on the map with larger variations than 1.92 (greater than two sigmas) reflect regions with potential provenance, lower than 5%.

REFERENCES

[1]. Spink, J. & Moyer, D. C. Defining the public health threat of food fraud. J. Food Sci. 76, R157–R163 (2011).
[2]. van Ruth, S. M., Huisman, W. & Luning, P. A. Food fraud vulnerability and its key factors. Trends Food Sci. Technol. 67, 70–75 (2017).
[3]. European Commission. Agri-food fraud. Agri-food fraud (2017). https://ec.europa.eu/food/safety/food-fraud_en.
[4]. Johnson, R. Food fraud and "Economically motivated adulteration" of food and food ingredients. Food Fraud Adulterated Ingre- dients Background, Issues, Fed. Action, 1–56 (2014).
[5]. Manning, L. Food fraud: policy and food chain. Curr. Opin. Food Sci. 10, 16–21 (2016).
[6]. PwC & SSAFE. Food fraud vulnerability assessment (2016).
[7]. European Commission. RASFF: The Rapid Alert System for Food and Feed 2017 Annual Report (2016).
[8]. Tähkäpää, S., Maijala, R., Korkeala, H. & Nevas, M. Patterns of food frauds and adulterations reported in the EU rapid alarm system for food and feed and in Finland. Food Control 47, 175–184 (2015).
[9]. Dasenaki, M. E. & Thomaidis, N. S. Quality and authenticity control of fruit juices—a review. Molecules 24, 1014 (2014).
[10]. Danezis, G. P., Tsagkaris, A. S., Camin, F., Brusic, V. & Georgiou, C. A. Food authentication: Techniques, trends & emerging approaches. TrAC - Trends Anal. Chem. 85, 123–132 (2016).
[11]. Camin, F. et al. Stable isotope techniques for verifying the declared geographical origin of food in legal cases. Trends Food Sci. Technol. https://doi.org/10.1016/j.tifs.2016.12.007 (2017).
[12]. Rossmann, A. Determination of stable isotope ratios in food analysis. Food Rev. Int. 9129, 347–381 (2001).
[13]. Rossmann, A. et al. Stable carbon isotope content in ethanol of EC data bank wines from Italy, France and Germany. Z. Lebensm. Unters. Forsch. 203, 293–301 (1996).
[14]. Gonzalvez, A., Armenta, S. & de la Guardia, M. Trace-element composition and stable-isotope ratio for discrimination of foods with Protected Designation of Origin. TrAC - Trends Anal. Chem. 28, 1295–1311 (2009).
[15]. Dansgaard, W. Stable isotopes in precipitation. Tellus 2826, 436–468 (1964).
[16]. Bowen, G. J. Isoscapes: Spatial pattern in isotopic biogeochemistry. Annu. Rev. Earth Planet. Sci. 38, 161–187 (2010).

[17]. Krouse, H. R. Sulfur Isotope Studies of the Pedosphere and Biosphere. In Stable Isotopes in Ecological Research (eds Rundel, P. W.
[18]. et al.) 424–444 (Springer, 1989). https://doi.org/10.1007/978-1-4612-3498-2_24.
[19]. Bateman, A. S., Kelly, S. D. & Woolfe, M. Nitrogen isotope composition of organically and conventionally grown crops. J. Agric. Food Chem. 55, 2664–2670 (2007).
[20]. Carter, J. F. & Chesson, L. A. Food Forensics: Stable Isotopes as a Guide to Authenticity and Origin. Food Forensics (CRC Press, 2017). https://doi.org/10.1201/9781315151649.
[21]. Epstein, S., Thompson, P. & Ya, C. J. Oxygen and hydrogen isotopic ratios in plant cellulose. Science (80-.) 198, 1209–1215 (1977).
[22]. Yakir, D. & DeNiro, M. J. Oxygen and hydrogen isotope fractionation during cellulose metabolism in Lemna gibba L. Plant Physiol.
[23]. 93, 325–332 (1990).
[24]. Sternberg, L., DeNiro, M. J. & Savidge, R. A. Oxygen isotope exchange between metabolites and water during biochemical reactions leading to cellulose synthesis. Plant Physiol. 82, 423–427 (1986).
[25]. Farquhar, G. D. & Lloyd, J. Carbon and Oxygen Isotope Effects in the Exchange of Carbon Dioxide Between Terrestrial Plants and the Atmosphere. In Stable Isotopes and Plant Carbon-Water Relations (eds Ehleringer, J. R. et al.) 47–70 (Academic Press, 1993). https://doi.org/10.1016/B978-0-08-091801-3.50011-8.
[26]. Roden, J. S., Lin, G. & Ehleringer, J. R. A mechanistic model for interpretation of hydrogen and oxygen isotope ratios in tree-ring cellulose. Geochim. Cosmochim. Acta 64, 21–35 (1999).
[27]. Yakir, D., DeNiro, M. J. & Gat, J. R. Natural deuterium and oxygen-18 enrichment in leaf water of cotton plants grown under wet and dry conditions: Evidence for water compartmentation and its dynamics. Plant Cell Environ. 13, 49–56 (1990).
[28]. Cernusak, L. A., Farquhar, G. D. & Pate, J. S. Environmental and physiological controls over oxygen and carbon isotope composi- tion of Tasmanian blue gum, Eucalyptus globulus. Tree Physiol. 25, 129–146 (2005).
[29]. Kahmen, A. et al. Effects of environmental parameters, leaf physiological properties and leaf water relations on leaf water δ18O enrichment in different Eucalyptus species. Plant Cell Environ. 31, 738–751 (2008).
[30]. Cueni, F., Nelson, D. B., Lehmann, M. M., Boner, M. & Kahmen, A. Constraining parameter uncertainty for predicting oxygen and hydrogen isotope values in fruit. J. Exp. Bot.
[31]. Harris, I., Osborn, T. J., Jones, P. & Lister, D. Version 4 of the CRU TS monthly high-resolution gridded multivariate climate dataset. Sci. Data 7, 1–18 (2015).
[32]. Cornes, R. C., van der Schrier, G., van den Besselaar, E. J. M. & Jones, P. D. An ensemble version of the E-OBS temperature and precipitation data sets. J. Geophys. Res. Atmos. 123, 9391–9409 (2017).
[33]. Bowen, G. J. Gridded maps of the isotopic composition of meteoric waters. (2015). http://www.waterisotopes.org. Accessed: 1st March 2015.